CHIMIA 1999, 53, No. 1/2

Chimia 53 (1999) 19–28

ISSN 0009–4293

From Catalyst Design to Molecular Devices: Theory and Experiments

Thomas R. Ward*, *Werner* Prize Winner 1998[a])

Abstract. Three different topics are presented herein. With the help of molecular-orbital analysis, the unique geometry and catalytic properties of d^0 bent-metallocenes was analyzed in search for cyclopentadienyl substitutes.

To overcome the inherent racemization of coordinatively unsaturated piano-stool complexes, a ten-electron donor ligand was designed. This ligand incorporates an arene bearing two tethers: a phosphine and an imine (abbreviated PArN). It was shown that upon η^6:η^1:η^1-coordination of PArN to ruthenium, a configurationally stable piano-stool complex results [Ru(η^6:η^1:η^1-PArN)L]$^{n+}$.

A tripodal dodecadentate ligand, incorporating three soft bipyridine donors as well as three harder salicylamide chelates, was synthesized. This ligand allowed the investigation of the iron release from ferric enterobactin, suggesting a protonation/translocation into a salicylate-binding mode. In the presence of a single iron ion and depending on its oxidation mode, it was shown that this system displays switch-like properties.

Foto: Rolf Häfliger

Thomas R. Ward was born in Fribourg on January 8th 1964 as the last of 6 children of *John E. Ward* and *Ada Lovinger Ward*. As an American citizen, he obtained Swiss nationality in 1976. He received his diploma in chemistry in 1987 from the University of Fribourg with organic chemistry as major and inorganic chemistry as minor subjects.

From 1988 to 1991, he was a doctoral student in the group of Prof. *L. M. Venanzi* at the ETH-Zürich. His PhD thesis dealt with the synthesis and coordination properties of C_3-symmetric phosphine ligands and their use as acetalization catalysts. This work benefited from a fruitful collaboration with Prof. *D. Seebach* as well as with *Ciba Geigy* which patented these systems.

Fascinated by group theory, he joined the group of Prof. *R. Hoffmann* at Cornell University as a *Swiss National Science Foundation* postdoctoral fellow (1991–1992). This theoretical excursion lead him into the fascinating field of heterogeneous catalysis: Why is rhodium so efficient at removing NO from car exhaust?

Soon after returning to Switzerland for a second postdoc in the group of Prof. *C. Floriani* at the University of Lausanne, he was awarded the *A. Werner* Fellowship and moved to Berne to undertake his independent career in Fall 1993.

1. Introduction

Catalysis is perhaps the word which best describes the spirit of chemistry: the miracle of consumption and regeneration [1]. Ever since my beginnings in science, I have been fascinated by all aspects of catalysis: bioinorganic, theoretical, organometallic, or as a tool to generate libraries [2].

After having identified a relevant problem from the current literature, I like to run qualitative molecular-orbital calculations to rationalize the published observations. Coincidentally, these form the basis for a synthetic project. Three distinct projects at different stages of achievement are presented herein: *i*) outlining a problem with the help of molecular orbital theory, *ii*) designing a ligand system, and, *iii*) applications.

2. The Geometry of d^0 Pentacoordinate Complexes [3]

2.1. *Background*

In the field of homogeneous catalysis, the most versatile catalysts may well be the so-called bent-metallocene systems. These contain a d^0-metal flanked by two cyclopentadienyls (abbreviated Cp). Most often, the catalyst precursors are $[MCp_2L_2]$-like compounds. If one considers Cp as a six-electron donor occupying a single coordination site, such complexes are four-coordinate, distorted tetrahedrons (T-4) with a large $Cp_{centroid}$–M–$Cp_{centroid}$ angle [4]. To understand their unrivalled catalytic properties, however, we focus on five coordinate $[MCp_2L_3]$-complexes. Pentacoordinate complexes play a pivotal role in transition-metal catalysis as five-coordinate transition states or intermediates have often been postulated either for associative reactions involving tetrahedral (T-4) or square planar (SP-4) complexes, or for dissociative reactions involving octahedral (OC-6) complexes [5].

The square pyramid (SPY-5) and the trigonal bipyramid (TB-5) represent prototypical geometries of five-coordinate complexes. The $[MCp_2L_3]$ compounds however cannot be categorized as either TB-5 or SPY-5. This is illustrated with three examples: $[TaCp_2H_3]$ **1** is one of the first structurally characterized $[MCp_2L_3]$ complexes [6]; $[ZrCp_2Cl(\eta^2\text{-}CH_3CO)]$ **2** is an early example of an η^2-bound acyl [7]; and **3** contains a planar four-coordinate carbon [8]. Interestingly, the proposed transition state **4** for the α-olefin polymerization catalyzed by bent metal-

*Correspondence: Dr. T.R. Ward
Department of Chemistry and Biochemistry
University of Berne
CH-3000 Berne 9
E-Mail: ward@iac.unibe.ch

[a]) See *Chimia* **1998**, *52*, 744.

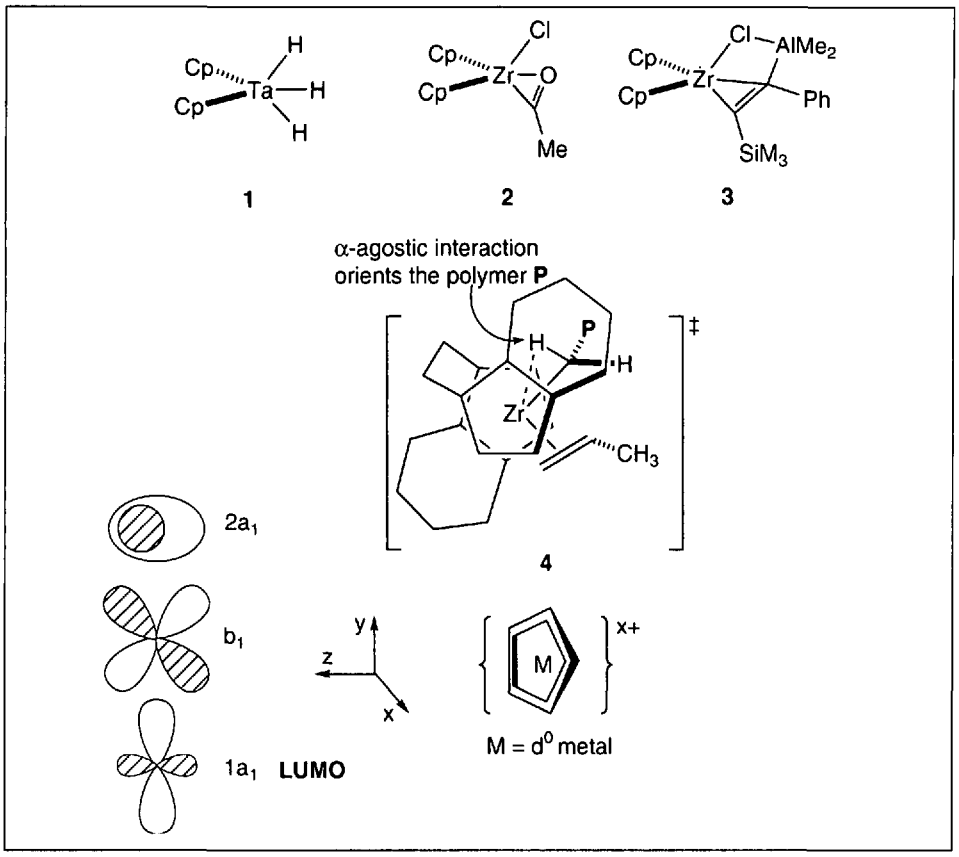

Fig. 1. *The three lowest-lying unoccupied orbitals of the bent d^0 {MCp_2} fragment dictate the coplanar arrangement of the {ML_3} fragment in [MCp_2L_3] complexes* **1–3** *and transition state* **5**

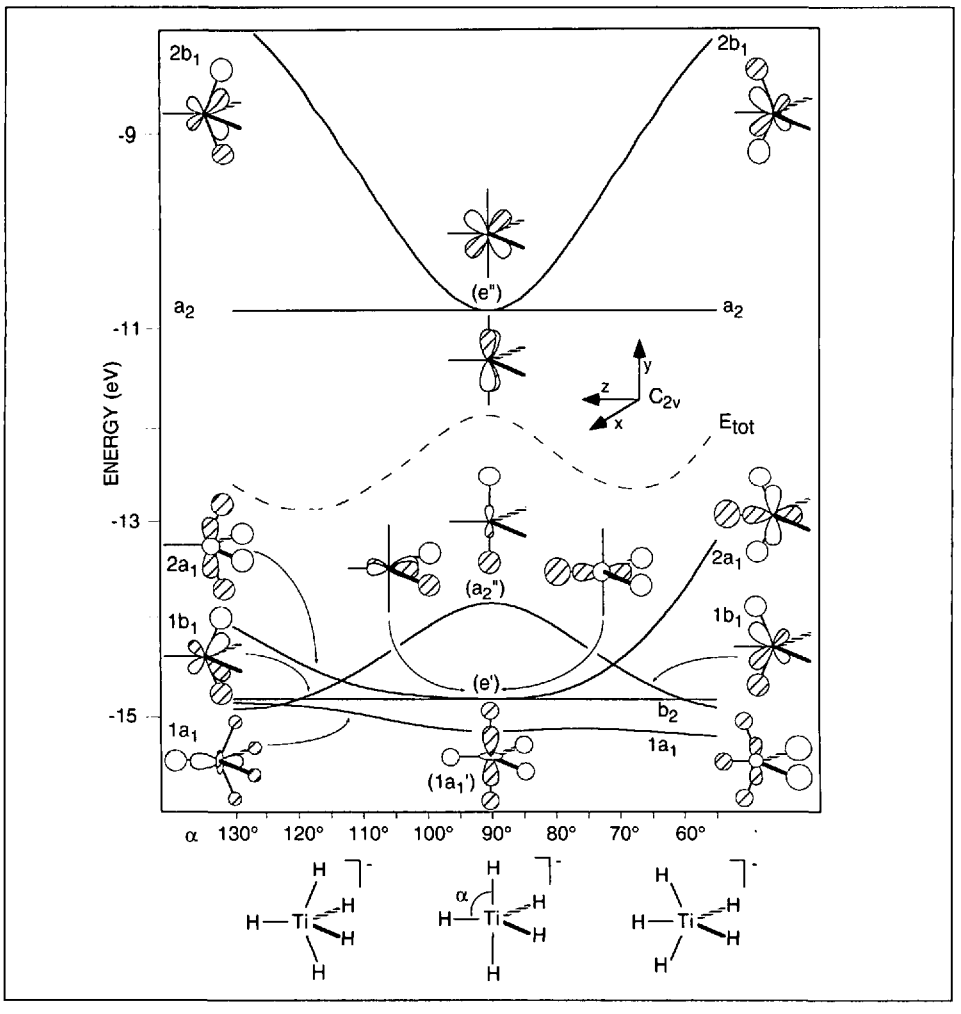

Fig. 2. Walsh *diagram for the SPY-5→TB-5→EBT-5 interconversion of* [TiH_5]$^-$. Dotted line : E_{tot}; labels in parentheses correspond to D_{3h} irreducible representations.

locenes also displays this unusual geometry. Structural features common to these complexes are a bent {MCp_2}-fragment and a coplanar arrangement of the three ligands L with two acute L–M–L angles. We call this unusual [MCp_2L_3] geometry 'edge-bridged tetrahedral', abbreviated as EBT-5 (*Fig. 1*).

We reasoned that perhaps the unique catalytic properties of bent-metallocene complexes may be related to their unusual EBT-5 geometry of their pentacoordinate complexes. We thus set out to analyze the electronic origin of this geometry, with the aim of finding Cp-substitutes which would also favor EBT-5 geometries.

2.2. *Theoretical Analysis*

2.2.1. *[TiH_5]$^-$*

We begin our analysis with an extended *Hückel* (e*H*) description of the bonding of a trigonal bipyramidal five-coordinate d^0 complex containing pure σ-donors. These qualitative arguments were assessed by Density Functional Theory (DFT). A simplified molecular-orbital diagram for a [TiH_5]$^-$ model is sketched in the middle of *Fig. 2*. The HOMO is a_2" and is mostly ligand-centered. The d_{xy} and d_{yz} orbitals remain unperturbed and correspond to the LUMO (e"). The second-order *Jahn-Teller* distortion (2OJTD) [9] of e' symmetry allows mixing of HOMO and LUMO's ($\Gamma_{HOMO} \otimes \Gamma_{LUMO} = a''_2 \otimes e'' = e'$). By varying the H_{piv}–Ti–H_{ax} angle α from 130° to 55°, we find two minima at 120° (E_{tot} = 0.00 eV) and 70° (E_{tot} = +0.22 eV) which correspond to the SPY-5 and EBT-5 geometries, respectively. The TB-5 (α = 90°, E_{tot} = +1.00 eV) is a transition state in this diagram. The SPY-5 *vs.* EBT-5 preference can be traced back to a difference in ligand-ligand interactions associated with the $2a_1$ orbital: artificially setting the L_{ax}–L_{eq} and L_{ax}–L_{piv} overlaps to zero reduces the energetic advantage of the SPY-5 over the EBT-5 to only 0.05 eV. It thus appears that the EBT-5 geometry is a result of a 2OJTD of e' symmetry. As the forward distortion ($\alpha > 90°$) presented in *Fig. 2*, corresponds to the *Berry* distortion, we suggest that the EBT-5 geometry results from a distortion along a reversed-*Berry* pathway.

Since the 2OJTD is doubly degenerate (e' symmetry), we must investigate a second distortion, also of e' symmetry. The α-distortion presented in *Fig. 2* corresponds to a rotation of both M–L_{ax} vectors around the x-axis. We investigate a β-distortion which corresponds to a rotation of both M–L_{ax} vectors around the y axis (see *Fig. 3*). The whole e' distortion pathway, was probed by independently varying $0° \leq \beta \leq$

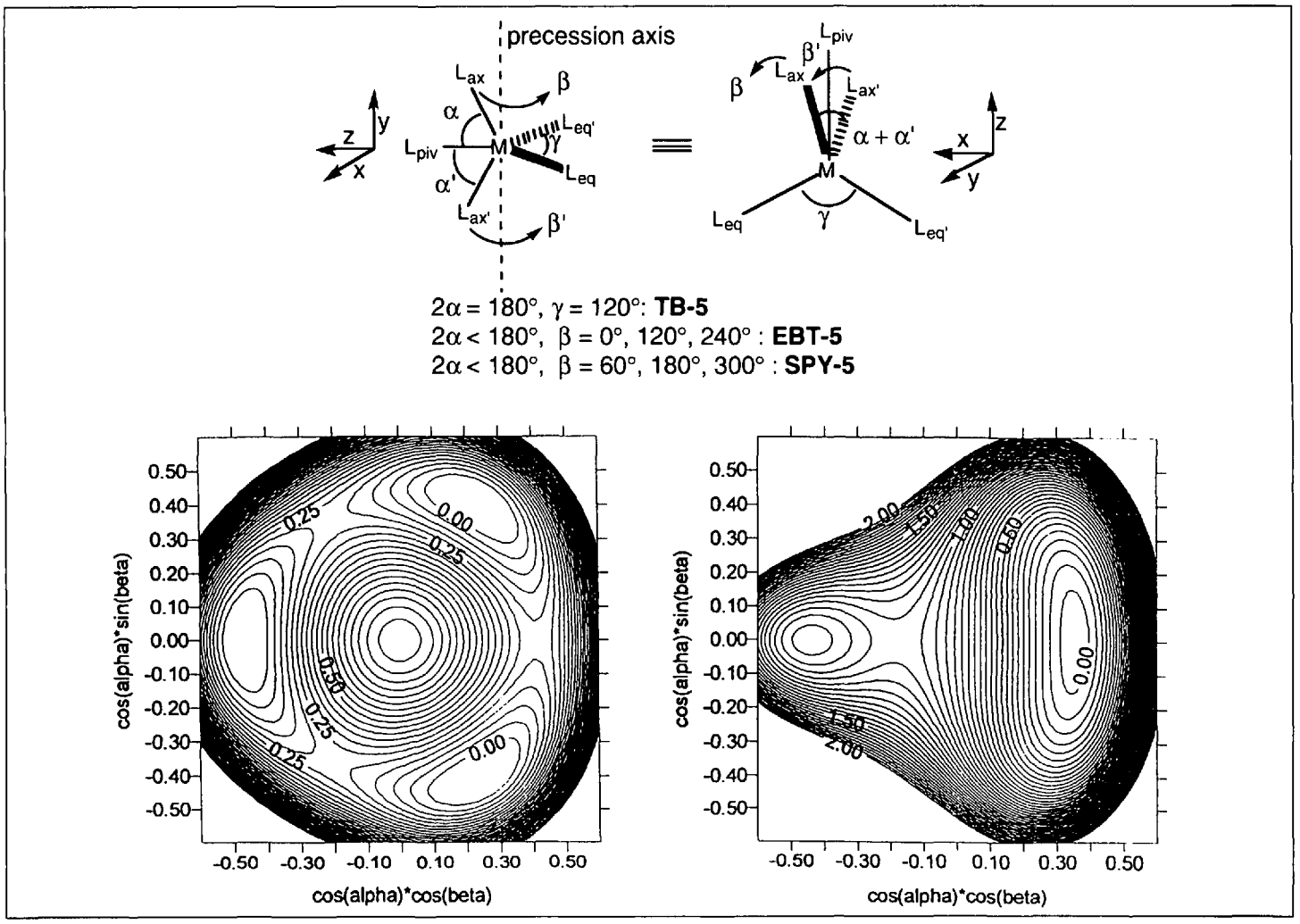

Fig. 3. *Potential-energy surface* E = *f*(α,β) *for the SPY-5→TB-5→EBT-5 interconversion of* $[TiH_5]^-$ (left) *and of* $[Ti(NH_2)_2H_3]^-$ (right). The coordinates, abscissa = cos α·cos β, ordinate = cos α·sin β, correspond to the position of an M–L_{ax} unit vector projected onto the *xz*-plane containing the $ML_{eq}L_{eq'}L_{piv}$ fragment, equienergy contours in eV.

360° and 55° ≤ α ≤ 90°. The resulting potential-energy surface (PES) is presented in *Fig. 3*, with ordinate cos α·sin β and abscissa cos α·cos β. These coordinates represent the projection of M–L_{ax} unit vectors onto the equatorial plane $ML_{eq}L_{eq'}L_{piv}$. This PES shows the expected Mexican-hat features with three minima and three saddle points corresponding to the SPY-5 (α = 60°, β = 60°, 180° and 300°) and EBT-5 (α = 70°, β = 0°, 120°, and 240°) geometries, respectively. The EBT-5 which appears as a minimum in the *Walsh* diagram *E* = f(α) (*Fig. 3*), is in fact a saddle point on the two-dimensional surface (*E* = f(α,β)) and lies well below the maximum representing the TB-5.

We conclude that a d^0 complex containing five pure σ-donors should display SPY-5 geometry. A Cambridge Structural Database (CSD) search revealed a single homoleptic compound containing five pure σ-donors around a d^0 metal: $[Ta(CH_2(4\text{-}MeC_6H_4))_5]$ [10]. This compound indeed displays an SPY-5 structure (2α = 138.1°, β = 177.2°). Recently, the structure of $[TaMe_5]$ was determined by gas-phase electron diffraction. In contrast to its main group counterpart $[SbMe_5]$, the d^0 complex has an SPY-5 geometry [11] [12].

As can be appreciated from *Fig. 2*, the total energy of the e'-distortion follows mostly the fate of the a_2'' orbital in D_{3h} symmetry (b_1 irreducible representation in C_{2v} point group). Introducing ligands capable of interacting with this orbital, which contains a large contribution of the d_{yz} orbital (in both C_{2v} geometries), may invert the SPY-5 preference, eventually leading to an EBT-5 ground state geometry.

2.2.2. $[Ti(NH_2)_2H_3]^-$

Adding two equatorial ligands capable of π-interaction, with their π-systems perpendicular to the equatorial plane fulfils this requirement: the in-phase combination of the two p_y orbitals is of b_1 symmetry. Let us replace two equatorial hydrides by two amides, with their p-orbital perpendicular to the *xz*-equatorial plane $[Ti(NH_2)_2H_3]^-$. The *Walsh* diagram for the α-distortion of $[Ti(NH_2)_2H_3]^-$ is presented in *Fig. 4*. As suspected, we compute the EBT-5 geometry (α = 70°, E_{tot} = 0.00 eV) to be preferred over the SPY-5 (α = 110°, E_{tot} = 0.91 eV), with a slightly distorted TB-5 (α = 95°, E_{tot} = 1.00 eV) as transition state.

Computing the PES *E* = f(α,β), we find an EBT-5 minimum, with a soft potential along the β-precession coordinate. This feature will be important in discussing experimental structural data (*Fig. 3b*).

Introduction of double-faced π-donor ligands (rather than the single-faced π-donors presented above) does not alter the overall picture. This can be traced down to the fact that the second π-interaction (typically a p_x orbital) does not have b_1 symmetry, and thus does not contribute significantly to the fate of the total energy in *Fig. 2*.

It thus appears that the geometry adopted by five-coordinate d^0-$[MD_2L_3]$ complexes with strong, single- or double-faced π-donors D as well as that adopted by $[MCp_2L_3]$ complexes is the result of the same 2OJTD along a reversed-*Berry* coordinate . From our model calculations, it

appears that *all* d^0 systems containing only two strong single-faced π-donors in the equatorial plane with their filled p orbital perpendicular to this plane (p_y) should display an EBT-5 geometry. In the following section, we test this model with structural data retrieved from the CSD.

2.3. *Structure Correlation*

2.3.1. *Fragment Definition*

In order to test the above hypothesis, we extracted all pentacoordinate d^0 complexes from the CSD. After defining and retrieving the structures of interest, we mapped the available structures in the two-dimensional configuration space spanned by α and β.

To ensure that the geometry is not biased by ligand constraints, all polynuclear complexes were excluded, as well as those containing chelating- or η^n-arene-ligands ($n > 1$). Only those compounds containing two strong π-donors were considered. To our surprise, this search yielded no more than seven pentacoordinated d^0-complexes containing *only* two strong π-donors.

Eventually, we relaxed our stringent definition to incorporate complexes which contain two strong π-donors and up to three weaker π-donors. A total of 36 complexes matched these requirements. These results are not presented here.

For comparison, all $[MCp_2L_3]$-like complexes were retrieved from the CSD. Again here, only mononuclear complexes and those containing no chelates were considered, yielding a total of thirteen $[MCp_2L_3]$-compounds.

2.3.2. *Ligand Labelling and Distortion Mapping*

To unambiguously determine the relevant distortion angles, a consistent ligand-labelling scheme is required. Since the complexes can be viewed as distorted TB-5, one large (< 180°), three medium (*ca.* 120°) and six small (*ca.* 90°) interligand angles are expected. After computing all ten interligand angles for each complex, the largest angle was assigned as the L_{ax}–M–$L_{ax'}$ angle. The remaining three ligands were taken to define the equatorial plane.

In those cases where two large angles (*ca.* 150°) were computed, thus suggesting an SPY-5 coordination, the equatorial plane was defined in terms of the two strongest π-donor ligands D and D' and the remaining equatorial ligand L_{piv}.

The observed structural data for $[MD_2L_3]$-complexes (D = strong π-donor, L = pure σ-donor) are displayed in *Fig. 5*, along with the e*H*-isoenergy contour at 0.1 eV for the model $[Ta(NH_2)_2H_3]^{2-}$. In most compounds of this class, the axial substituents bend away from the π-donors and towards the pivot ($2\alpha < 180°$ and $\beta < 30°$). Five of the seven compounds are within the minimum-energy region calculated for the model complex $[Ta(NH_2)_2H_3]^{2-}$.

Inspection of $[Ta(CHBu^t)_2Mes(PMe_3)_2]$ (*Entry 1*), reveals an EBT-5 geometry. The presence of a very bulky mesitylene in the pivot position, prevents an efficient 2OJTD resulting in a large α-angle ($2\alpha = 166.3°$).

Systems incorporating one strong and one weaker π-donor can be expected to adopt geometries intermediate between EBT-5, encountered with 2 strong π-donors, and SPY-5, a geometry prevalent with pentacoordinate compounds bearing a single π-donor [13][14]. Such an intermediate geometry is observed not only for $[ReO_2(Np)_3]$ (*Entry 4*) but also for $[WO(NEt_2)Np_3]$ (*Entry 7*) [15]. In both cases, the axial ligands precess towards the weaker π-donor, the longest, most distant oxo- and the amide-groups, respectively.

For $[MCp_2L_3]$ complexes, the 2α angles fall in the range 148.0–102.1°. It is interesting to note that the complexes which are least bent are those with the most electronegative L_{ax}. Electropositive axial donors favour the 2OJTD since in the TB-5 geometry, the HOMO is essentially located on the axial donor ligands (see *Fig. 2*). Good axial donors raise the energy of this orbital, and thus favor an efficient 2OJTD as this latter is inversely proportional to the HOMO-LUMO gap. This is nicely reflected with compounds containing axial silanes which all display very acute L_{ax}–M–$L_{ax'}$ angles, despite significant steric interactions with L_{piv}.

It should be noted that the minimum computed for our model $[TaCp_2H_3]$ is very deep and small distortions both in the

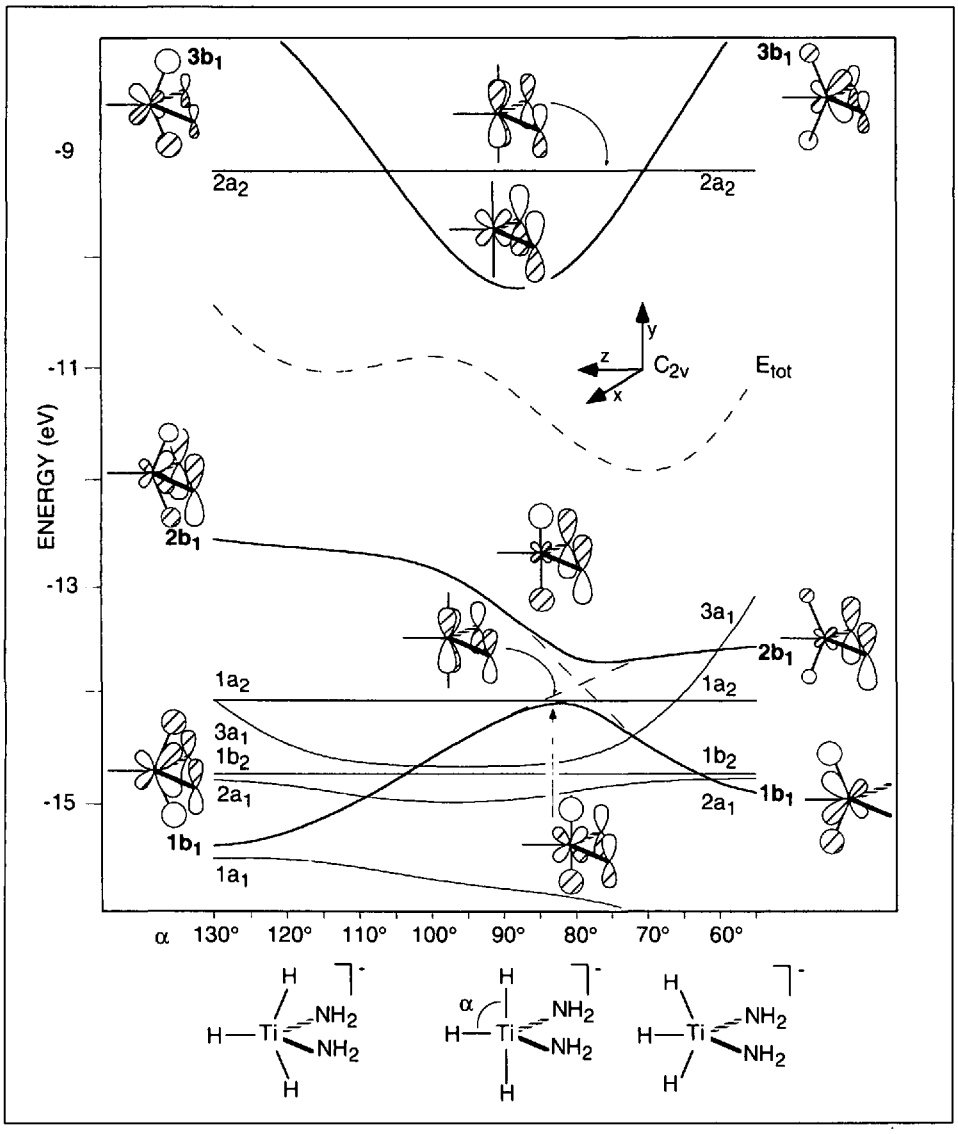

Fig. 4. Walsh *diagram for the SPY-5→TB-5→EBT-5 interconversion of* $[Ti(NH_2)_2H_3]^-$. Only the MOs containing Np_y contributions are sketched. All other MOs are very similar to those of *Fig. 2* (Dotted line: E_{tot}).

α and β directions are costly in energy. The distortion along the β coordinate is disfavoured purely on steric grounds: at $\alpha = 65°$ and $\beta = 30°$, the shortest H_{ax}–H_{Cp} and H_{ax}–C_{Cp} contacts are 2.05 Å and 2.02 Å respectively. By artificially setting the H_{ax}–H_{Cp} and H_{ax}–C_{Cp} overlaps to zero, the shallow minimum observed for $[Ti(NH_2)_2H_3]^-$ in EBT-5 is restored and the β-precession about the y-axis is soft.

2.4. *Outlook*

A theoretical analysis has revealed that the EBT-5 geometry of d^0 bent metallocenes $[MCp_2L_3]$ is the result of a reversed-*Berry* distortion. Such EBT-5 geometries are predicted for all five coordinate d^0 complexes which incorporate two strong π-donors. Our theoretical model was tested with a structure-correlation analysis of all d^0 five-coordinate complexes incorporating two strong π-donors.

In the spirit of *Muetterties* and *Guggenberger*'s mapping of the *Berry* pathway [16] the d^0 complexes containing two π-donors can be arranged in a sequence that maps a reversed-*Berry* pathway (*Fig. 7*).

Based on this study, we predicted that d^0 bis-amide-systems should display bent-metallocene-like catalytic properties. We were pleased to see that such systems reported by *McConville*, *Schrock* and *Gibson* indeed display very promising olefin-polymerization properties [17–19].

3. Synthesis of Configurationally Stable Three-Legged Piano-Stool Complexes [20]

3.1. *Background*

In the field of enantioselective transition-metal catalysis, ligand design plays a very prominent role. In the spirit of *E. Fischer*'s 'lock and key' concept, the steric bulk on the chiral ligand is relayed by a metal template to a prochiral substrate, eventually giving rise to chiral induction. To simplify matters, C_2-symmetric bidentate ligands were tailored, reducing the number of diastereomers from four to two upon complexation of a prochiral substrate.

In the early nineties, however, electronically asymmetric bidentate ligands were introduced and rapidly found many applications in enantioselective catalysis [21–23]. In such systems, in addition to steric arguments, *electronic factors* play a critical role in determining which diastereoisomer (or diastereoisomeric site) reacts *faster* to yield the enantiomerically enriched product. Such C_1-symmetric bi-

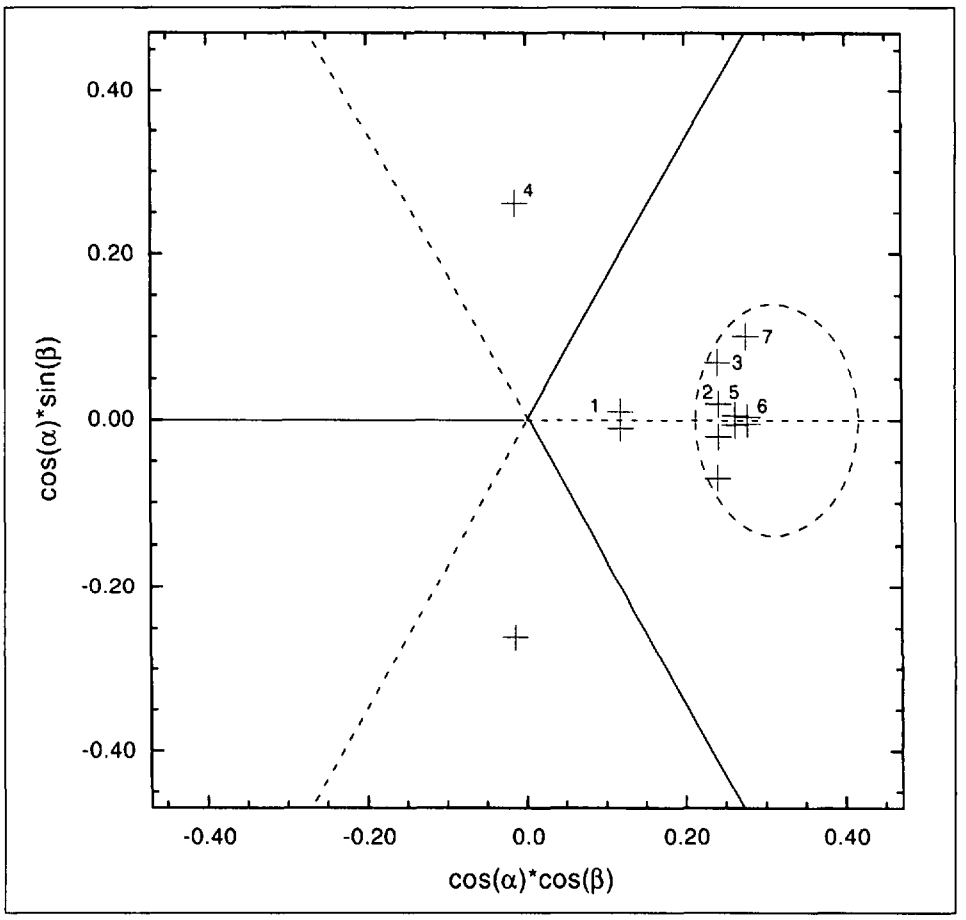

Fig. 5. *Mapping of $[MD_2L_3]^{x-}$ structures (D = strong π-donor, L = pure σ-donor).* The dotted circular line represents the 0.1 eV e*H* isoenergy contour computed for $[Ta(NH)_2H_3]^{2-}$ (Definition of coordinates, see *Fig. 3*).

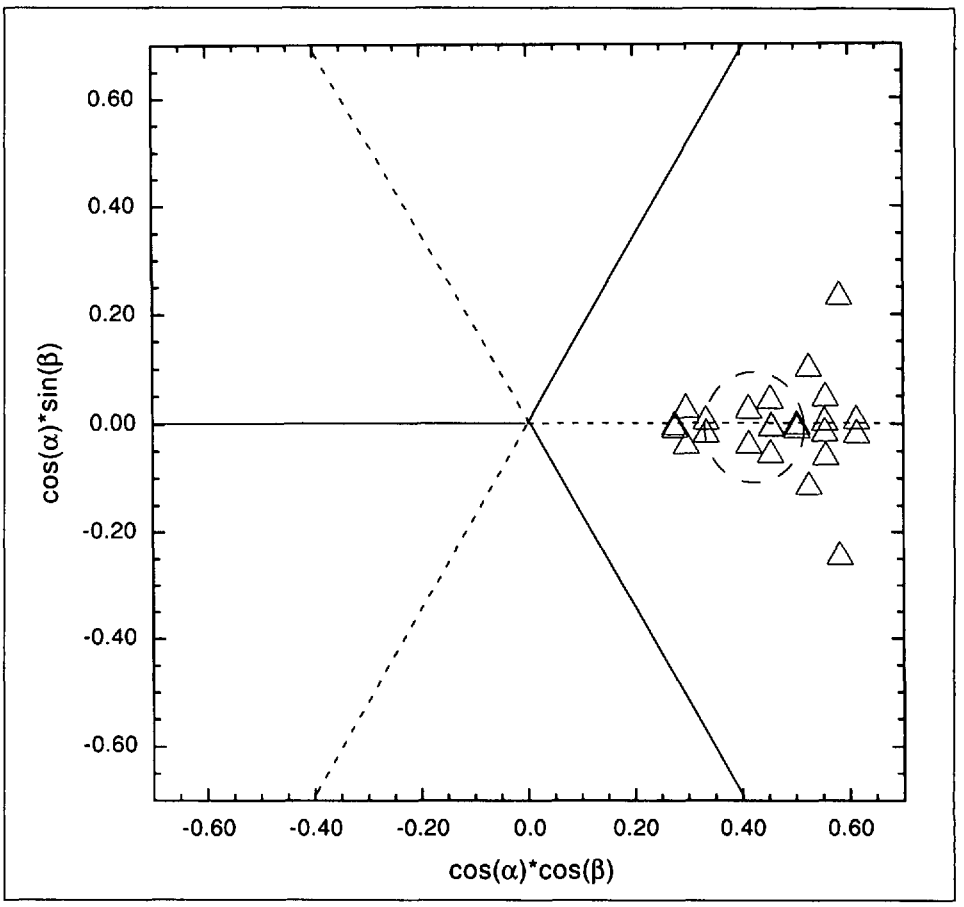

Fig. 6. *Mapping of $[MCp_2L_3]^{x-}$ structures.* The dotted circular line represents the 0.1 eV e*H* isoenergy contour computed for $[TaCp_2H_3]$ (Definition of coordinates, see *Fig. 3*).

dentate ligands offer the interesting prospective of studying the role of metal-based chirality. To our knowledge, this area has received only little attention, despite interesting preliminary reports.

As early as 1979, *Faller et al.* reported a chiral molybdenum-based promoter **5** for the functionalization of allylic substrates [24]. It was shown that, when coordinated to the $[CpMo(CO)(NO)]^+$-moiety, a symmetric allyl could be functionalized diastereoselectively at the carbon *cis*-positioned to the nitrosyl in the *exo*-conformation [25]. As a nitrosyl ligand is as bulky as a carbonyl ligand, there remains little doubt that the diastereoselectivity must be caused by electronic rather than steric arguments. Unfortunately, however, the system was stoichiometric and not catalytic. Similarily, *Gladysz* has extensively studied the *Lewis*-acidic $[ReCp(NO)PPh_3]^+$ fragment **6** as a promoter for functionalizing prochiral substrates [26]. Again here, only stoichiometric applications have been reported.

One possible explanation for this fact could well be the configurational lability of the coordinatively unsaturated piano-stool complexes which are invariably involved in catalytic cycles. If a chiral-at-metal complex were to racemize during catalysis, this would have a dramatic effect on the enantiomeric excess of the reaction.

Before studying the role of chirality-at-the-metal in enantioselective catalysis, we analyzed theoretically the role of electronic asymmetry in the palladium-catalyzed allylic alkylation as well as the geometry of coordinatively unsaturated two-legged piano-stool complexes. Based on these results, we designed a chiral-at-metal piano stool complex which displays remarkable configurational stability.

3.2. *Theoretical Considerations* [27]

3.2.1. *On the Regioselectivity of a Nucleophilic Attack on [Pd(allyl)(phosphine)(imine)] Complexes*

To understand the role of electronic asymmetry, we analyzed the frontier orbitals of a model $[Pd(\eta^3\text{-}C_3H_5)(PH_3)(NH_2)]$. We reasoned that since the coordinated allyl fragment undergoes a nucleophilic attack, the carbon atom which bears the greatest coefficient in the LUMO is most prone to be functionalized by the incoming soft nucleophile. The interaction diagram for $[Pd(\eta^3\text{-}C_3H_5)(PH_3)(NH_2)]$ is built from the $\{Pd(PH_3)(NH_2)\}^+$ and $(\eta^3\text{-}C_3H_5)^-$ (see *Fig. 8*).

The LUMO of such systems consists essentially of the out-of-phase combination of the $d_{x^2-y^2}$ with the non-bonding orbital of the allyl π-system. Close inspection of the $d_{x^2-y^2}$ orbital of $\{Pd(PH_3)(NH_2)\}^+$, however, reveals that this Fragment Molecular Orbital (FMO) is hybridized away from the nitrogen, a mere reflection of the electronic asymmetry caused by the P^N ligand. This hybridization allows mixing of both the π and π^* orbitals of the allyl-fragment into the LUMO as their overlap with the hybridized $d_{x^2-y^2}$ orbital is no longer zero. Because of the good energy match between the π^* and the LUMO, only this orbital contributes (and not the π orbital) significantly to the LUMO. Perturbation theory allows to predict that

$$LUMO \propto d_{x^2-y^2} - (n) + (\pi^*)$$

As can be appreciated from *Fig. 8*, the $C_{trans\text{-}P}$ bears the greatest coefficient and thus is predicted to be most electrophilic. It should be pointed out that this picture is independent of the allyl conformation (*exo* or *endo*). As both these conformations interconvert rapidly under true catalysis conditions, we conclude that the nucleophile attacks preferentially the $C_{trans\text{-}P}$ of the *exo*-conformation, yielding the observed enantiomer. This prediction was subsequently substantiated by DFT methods [28][29].

Qualitative MO arguments thus help rationalize the role of electronic asymmetry in enantioselective catalysis. Similar arguments were used with *Faller*'s piano-stool complex $[CpMo(CO)(NO)(\eta^3\text{-allyl})]$ **5** to rationalize the site of nucleophilic attack on the coordinated allyl [25].

3.2.2. *Geometry of Coordinatively Unsaturated Two-Legged Piano-Stool Complexes* [30]

Following the synthesis of chiral-at-metal piano-stool complexes, initiated by *Brunner et al.*, the question of configurational stability of such systems was addressed by various groups [31]. Of particular interest in the context of catalysis are coordinatively unsaturated piano-stool complexes as these would be invariably involved in a catalytic cycle involving piano-stool complexes as catalysts.

It had been suggested by *Hofmann* that 16-electron complexes of the type $[M(\eta^n\text{-}C_nH_n)LL']$ ($n = 4$–7) may have pyramidal and thus chiral-at-metal ground-state geometries [32]. Twenty years later, no firm experimental proof unambiguously validated this prediction. We thus re-analyzed these systems, in search of more quantitative predictions, *i.e.*, inversion barriers.

Our calculations suggest that, indeed, coordinatively unsaturated two-legged pi-

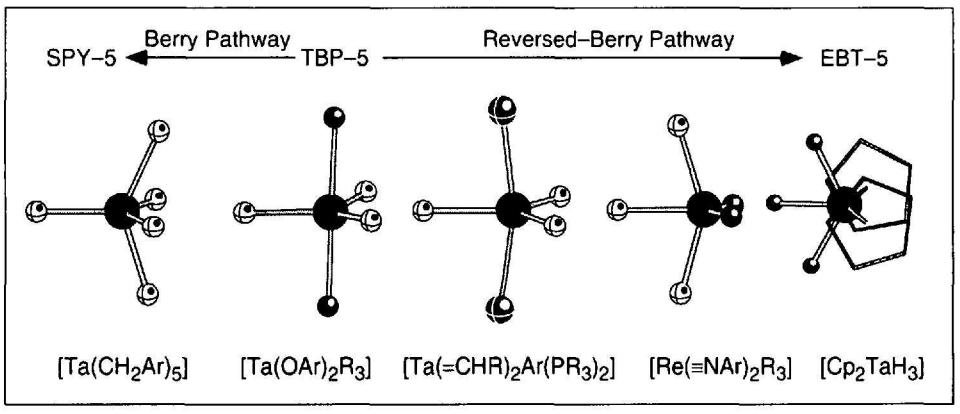

Fig. 7. *Mapping of the reversed-*Berry *pathway with five-coordinate d^0 complexes incorporating two π-donors and three σ-donors*

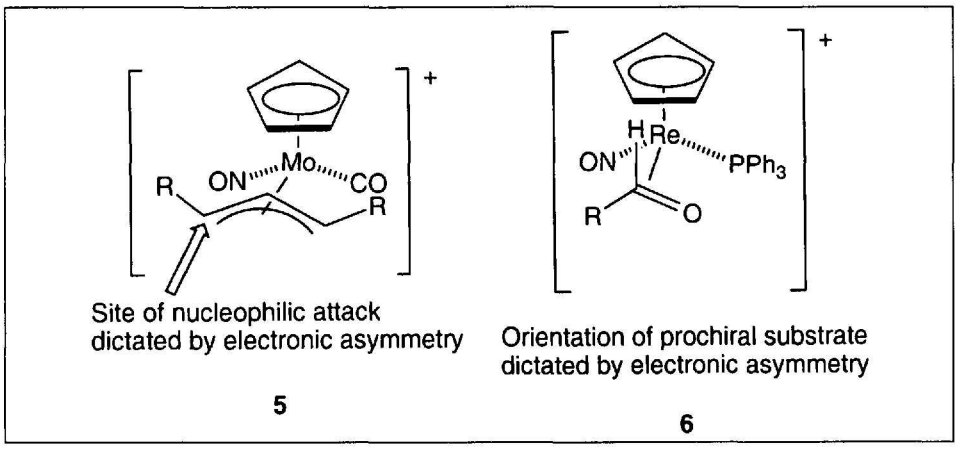

ano-stool complexes possess a pyramidal ground-state geometry. In all cases, however, the inversion barriers, *via* a planar, achiral geometry are low. The best candidate, $[FeCp(NO)SiR_3]^+$, incorporates an electropositive σ-donor (SiR_3) and an excellent π-acceptor (NO^+). Unfortunately, its inversion barrier is computed at 15 kcal·mol^{-1} and thus is expected to readily racemize in solution at room temperature. Such systems have much in common with amines, which are pyramidal, but readily racemize in solution as their inversion barriers are low in most cases.

For both *N*-based and metal-based chirality, the pyramidalization is caused by a 2OJTD away from the planar achiral geometry. For *N*-based chirality, electronic tuning of the substituents on nitrogen (*i.e.*, electronegative substituents or incorporation into a small ring) suffices to prevent rapid racemization. Incorporation of the nitrogen in a bicyclic framework locks the configuration and allows the separation of enantiomers. This was elegantly achieved with the resolution of *Tröger*'s base by *Prelog* [33].

We reasoned that tethering of two donors on an arene would yield, after $\eta^6{:}\eta^1{:}\eta^1$-coordination to a metal center, a bicyclic-like framework, and thus prevent racemization (see *Fig. 9*).

3.3. *Synthesis and Characterization of a Configurationally Stable Piano-Stool Complex* [34]

Having analyzed in detail phosphine-imine systems (*vide supra*), we set out to synthesize a ten-electron donor ligand incorporating an electron deficient imine and a phosphine tethered to an arene (abbreviated PArN). The ligand synthesis as well as its coordination to ruthenium are summarized in *Fig. 10*. After $\eta^6{:}\eta^1$-coordination, a racemic, planar chiral complex $[Ru(\eta^6{:}\eta^1\text{-PArN})Cl_2]$ (**8**) was obtained. After many unsuccessful derivatization- and crystallization experiments, we were pleased to find that the racemate could be resolved by preparative HPLC on *Chiralpak AD* using EtOH, to afford both enantiomers in nearly quantitative yield. Chloride abstraction in a coordinating solvent yields the chiral-at-metal complex $[\{\eta^6{:}\eta^1{:}\eta^1\text{-(PArN)}\}Ru(OH_2)](OTf)_2$ **9** which displays remarkable configurational stability. Its X-ray structure is depicted

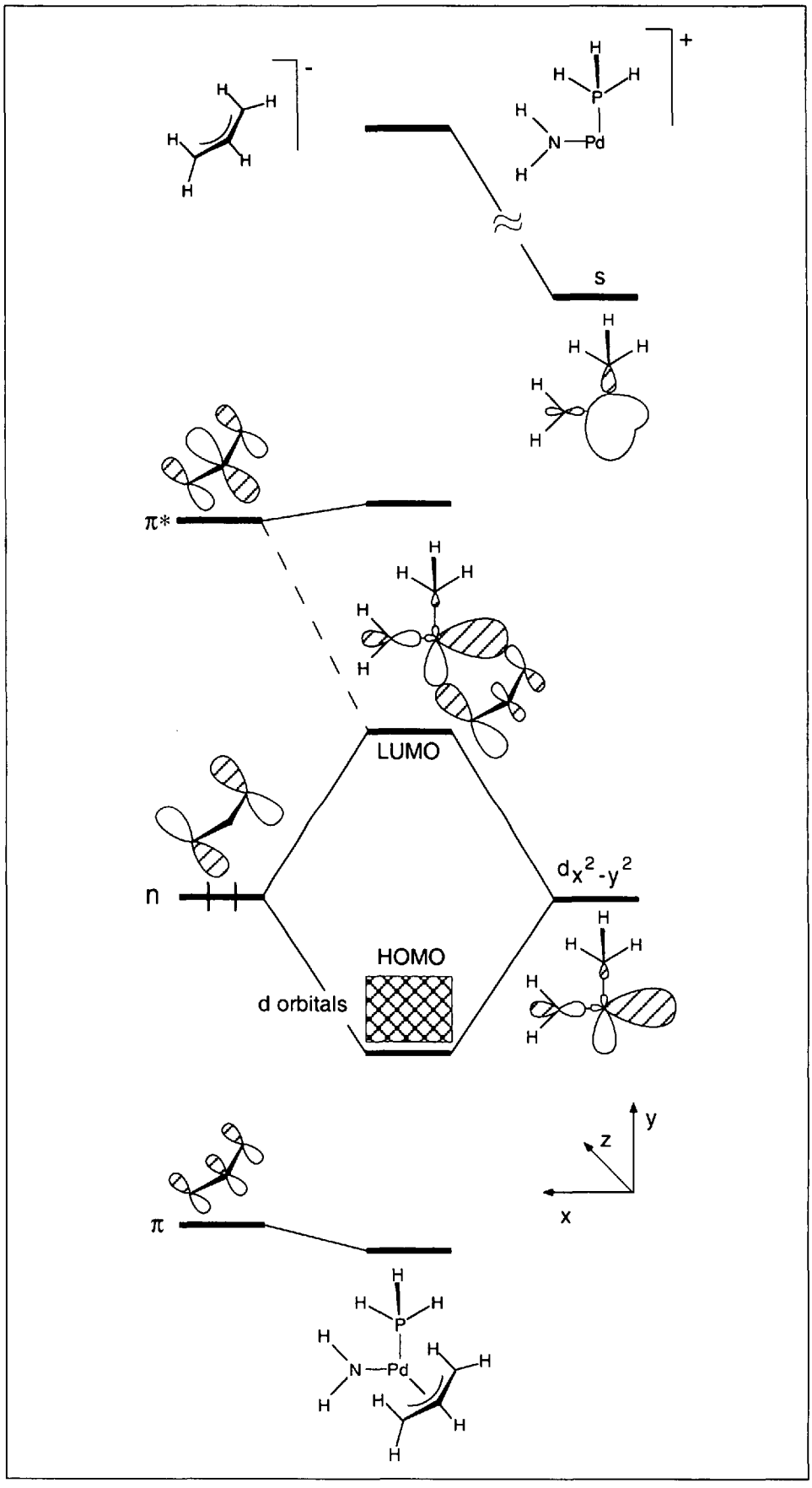

Fig. 8. *Simplified interaction diagram between* $\{Pd(NH_2)PH_3\}^+$ *and* $(C_3H_5)^-$

3.4. *Outlook*

Based on two theoretical analyses addressing the role of electronic asymmetry in enantioselective catalysis and the geometry of coordinatively unsaturated piano-stool complexes, we have synthesized a configurationally stable three-legged piano-stool complex which displays promising catalytic activities in various C–C-bond forming reactions (*i.e.*, *Mukaiyama* aldol, *Diels-Alder* reaction and cyclopropanation). Although a considerable effort may be required to optimize the ligand design to obtain excellent levels of induction, we have shown that such systems are amenable to address the role of chirality at the metal in enantioselective catalysis.

4. An Iron-Based Molecular Switch [35]

4.1. *Background*

Once upon a time, *ca.* 2.5 billion years ago, the atmosphere surrounding the Earth contained very little dioxygen (< 1%). As a consequence, the first multimolecular units were anaerobic and used the surrounding organic compounds as the source of building materials and energy. Gradually, the primordial soup depleted. Photosynthetic cells using light as an energy source may well have been the response to the dearth of energy [36]. The remarkable ability of these primitive organisms to switch to the use of H_2O as a reductant, with the concomitant production of dioxygen, probably produced the worst case of pollution in terrestrial history. Indeed, the photosynthesis reaction (*Eqn. 1*) produces carbohydrates, essential feedstocks for higher organisms, as well as equimolar amounts of dioxygen as a by-product:

$$n\,CO_2 + n\,H_2O \xrightarrow[\text{catalyst}]{h\nu} (CH_2O)_n + n\,O_2 \quad (1)$$

Long before the appearance of dioxygen, organisms had developed an addiction to iron for various purposes. The choice of iron may well be due to its abundance (fourth most abundant element in earth's crust) as well as its versatility as a catalyst thanks to its broad range of accessible oxidation states. Photosynthetic activity dramatically decreased the availability of iron in water, as dioxygen oxidizes iron to its ferric state with subsequent production of rust as illustrated in (*Eqn. 2*):

$$4\,Fe + 3\,O_2 + 6\,H_2O \rightarrow 4\,Fe(OH)_3 \rightarrow \text{RUST} \quad (2)$$

Thereafter, the dioygen concentration in the atmosphere rose steadily and stabilized at about 20%, *ca.* 300 million years ago [37]. This elicited the appearance of aerobic cells that could not only withstand this pollution but could even turn it to their advantage by developing respiratory and oxidative processes capable of extracting energy more completely from nutrient molecules.

Paradoxically, the iron required as catalyst for photosynthesis became scarce because this reaction produces dioxygen and indirectly rust. Hard-pressed organisms eventually came up with an elegant solution to this threat. Iron-scavenging agents, referred to as siderophores, were released by organisms to collect the vital metal. Siderophores are chelating ligands which display very high affinity for iron. Typically, the binding constants of these ligands are higher than the solubility product of rust under physiological conditions, allowing siderophores to extract ferric ions from rust.

Almost all bacteria and fungi secrete low-molecular-weight siderophores to scavenge iron from their environment. Most natural and synthetic siderophores contain either three hydroxamate- or three catechol-binding sites. Enterobactin, a triscatecholate ligand, is the most powerful natural siderophore known to date with an overall stability constant of *ca.* 10^{49}. With such high binding constants, the iron-release mechanism has attracted considerable attention [38].

To simulate the iron-uptake and -release mechanism, we designed a dodecadentate ligand which mimics both a siderophore with high affinity for a hard ferric ion as well as an 'octahedral, por-

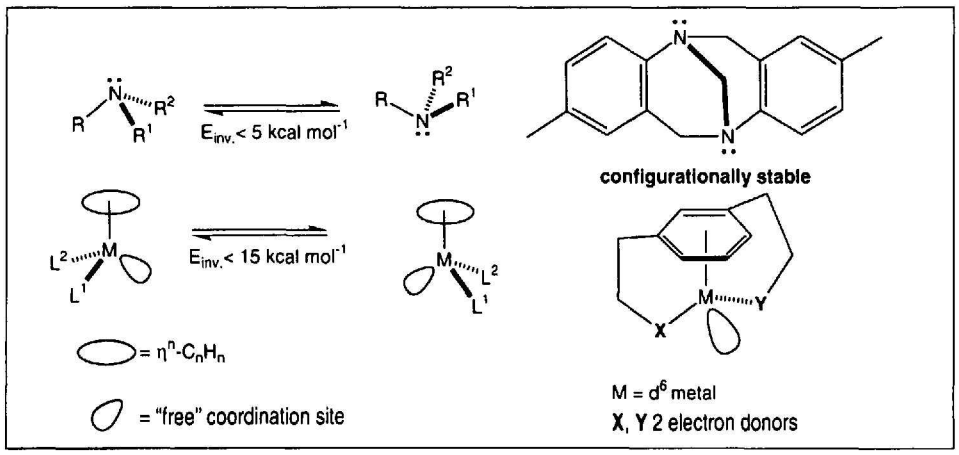

Fig. 9. *Anchoring a configurationally labile chiral center in a bicyclic framework results in a configurationally stable complex*

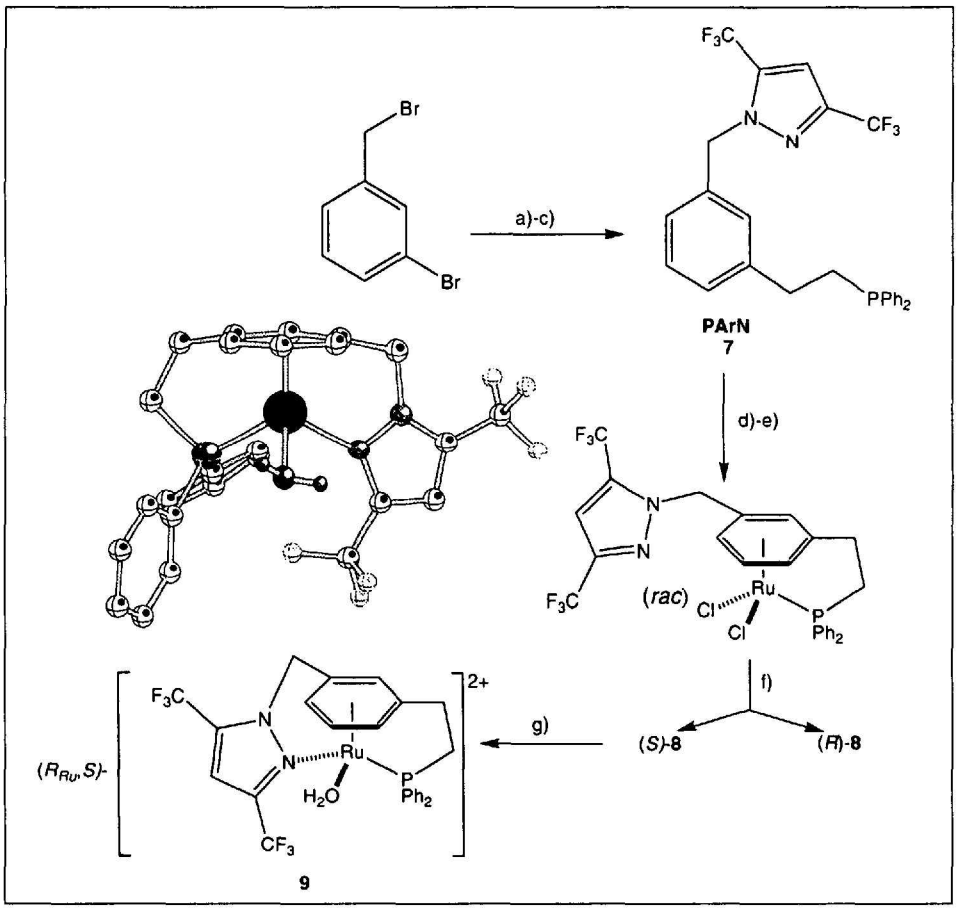

Fig. 10. *Preparation and structural characterization of the enantiomerically pure complex* $[\{\eta^6{:}\eta^1{:}\eta^1\text{-}(PArN)\}Ru(OH_2)](OTf)_2$ **9**. *a)* 3,5-Bis(trifluoromethyl)pyrazole, NaH, DMF, r.t., 2 h then 60° 48 h (86%); *b)* [Pd(PPh3)4], $Bu_3Sn(CHCH_2)$, Toluene, 100°, 8 h (92%); *c)* $HPPh_2$, AIBN, CH_2Cl_2, $h\upsilon$ (quant.); *d)* 0.5 equiv. $[(\eta^6\text{-}C_6H_5CO_2Et)RuCl_2]_2$, CH_2Cl_2, r.t., 0.5 h (82%); *e)* CH_2Cl_2, 110°, 24 h (quant.); *f)* HPLC on *Chiralpak AD*, EtOH ; *g)* excess $CF3SO_3Ag$, THF/H_2O (quant.).

phyrin-like environment' to accommodate the softer ferrous ion [39][40]. We reasoned that in the presence of a single iron ion and depending on its oxidation state, the metal ion would bind selectively to one site or the other. Oxidation or reduction could be used to drive the metal reversibly and intramolecularly from one site to the other, as schematized in below:

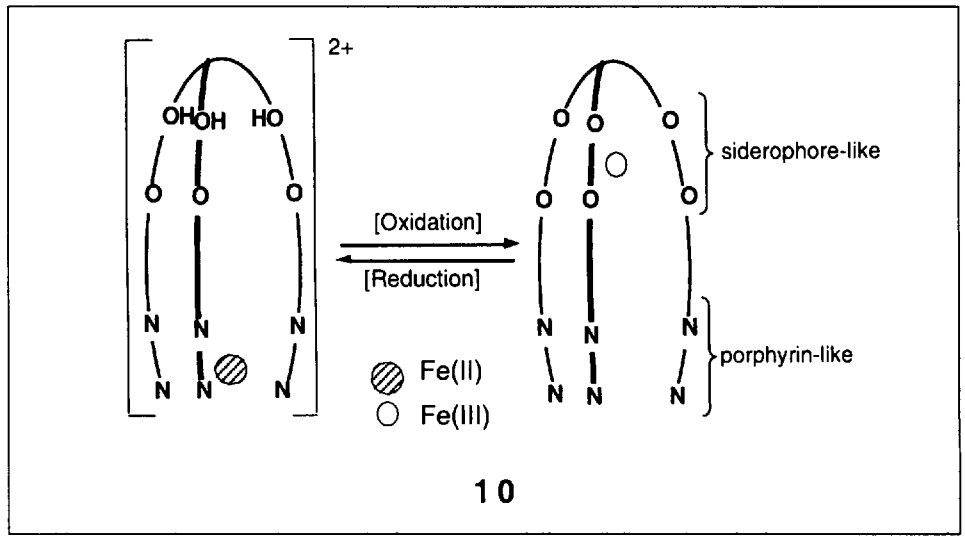

10

4.2. *Results and Discussion*

In contrast to hydroxamate-based siderophores, and due to its stability, the reduction potential of [Fe(III)(enterobactin)]$^{3-}$ lies outside the range accessible with natural reducing agents (*i.e.*, NADH and $FADH_2$) [41]. Therefore, alternative release mechanisms have been investigated for [Fe(III)(enterobactin)]$^{3-}$. The main pathway seems to occur *via* a hydrolysis of its tris-lactone backbone. An interesting alternative is a protonation of a catechol oxygen with a concomitant translocation in a 'salicylate-binding mode' [42].

To probe this, we synthesized a tripodal dodecadentate ligand consisting of three salicylamide-binding sites and three electron-deficient 2,2'-bipyridines (abbreviated $(NNOO)_3$. With this ligand at hand, we showed that these systems are coded for the oxidation-state-selective iron chelation and iron transport. The low-spin ferrous ion binds selectively to the soft tris-bipyridine pocket $[Fe(II)(\mathbf{NNOO})_3]^{2+}$, while the high-spin ferric ion binds to the harder tris-salicylamide pocket $[Fe(III)(\mathbf{NNOO})_3]$. Moreover, it was observed that oxidation or reduction induces intramolecular (depending on conditions), reversible iron translocation between these two sites, thus revealing switch-like properties. This is best illustrated with visible spectra resulting from the titration of the ferric complex $[Fe(III)(\mathbf{NNOO})_3]$ with aliquots of aqueous vitamin C resulting in the formation of the ferrous complex $[Fe(II)(\mathbf{NNOO})_3]^{2+}$ (see *Fig. 11*). Alternatively the ferrous complex may be oxidized with H_2O_2 to yield the ferric complex. These two series of spectra are superimposable.

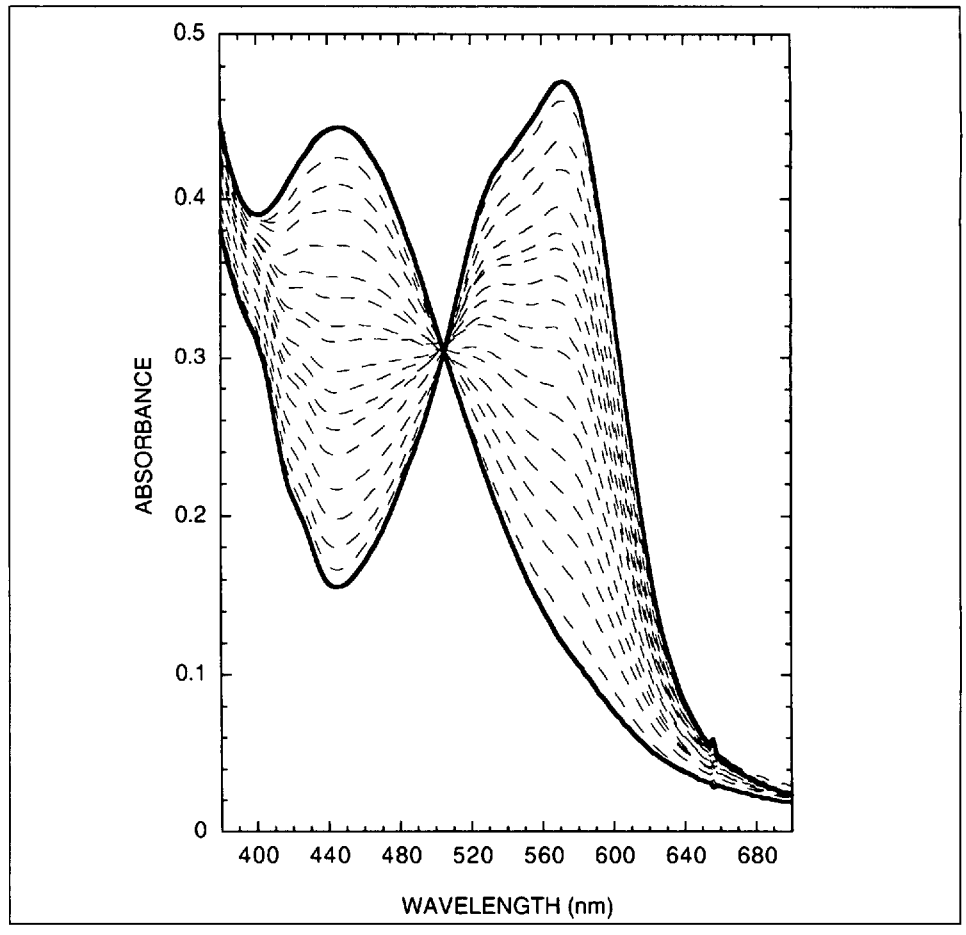

Fig. 11. *Visible-absorption spectra resulting from the treatment of the ferric complex* $[Fe(III)(\mathbf{NNOO})_3]$ (λ_{max} = 460 nm) *with vitamin C yielding the ferrous complex* $[Fe(II)(\mathbf{NNOO})_3]^{2+}$ (λ_{max} = 575 nm)

4.3. *Outlook*

The iron localization, oxidation state and translocation are conveniently addressed by visible spectroscopy. Furthermore, the *Mössbauer* spectrum for the ferric complex is fully consistent with that obtained by *Raymond* upon lowering the pH of [Fe(III)(enterobactin)]$^{3-}$ solutions, thus supporting the iron-release mechanism from enterobactin *via* the salicylate-binding mode [42]. A summary of the spectroscopic data is presented in *Fig. 12*.

5. Conclusions

Three different projects were outlined in this paper:

- *i) What makes d^0 bent-metallocenes so unusual?*
  A MO analysis, coupled with a structure correlation revealed that $[Cp_2ML_3]$ complexes can be viewed as trigonal bipyramidal structures which undergo distortion along a reversed-*Berry* pathway. Given the right electronic environment, this distortion is energetically favoured over the *Berry* distortion and is in fact quite common. Extensions of this work to metals with different electron counts as well as the synthesis of novel cyclopentadienyl substitutes are planned [43].
- *ii) What is the role of metal-based chirality in enantioselective catalysis?*
  To probe this question, we developed a

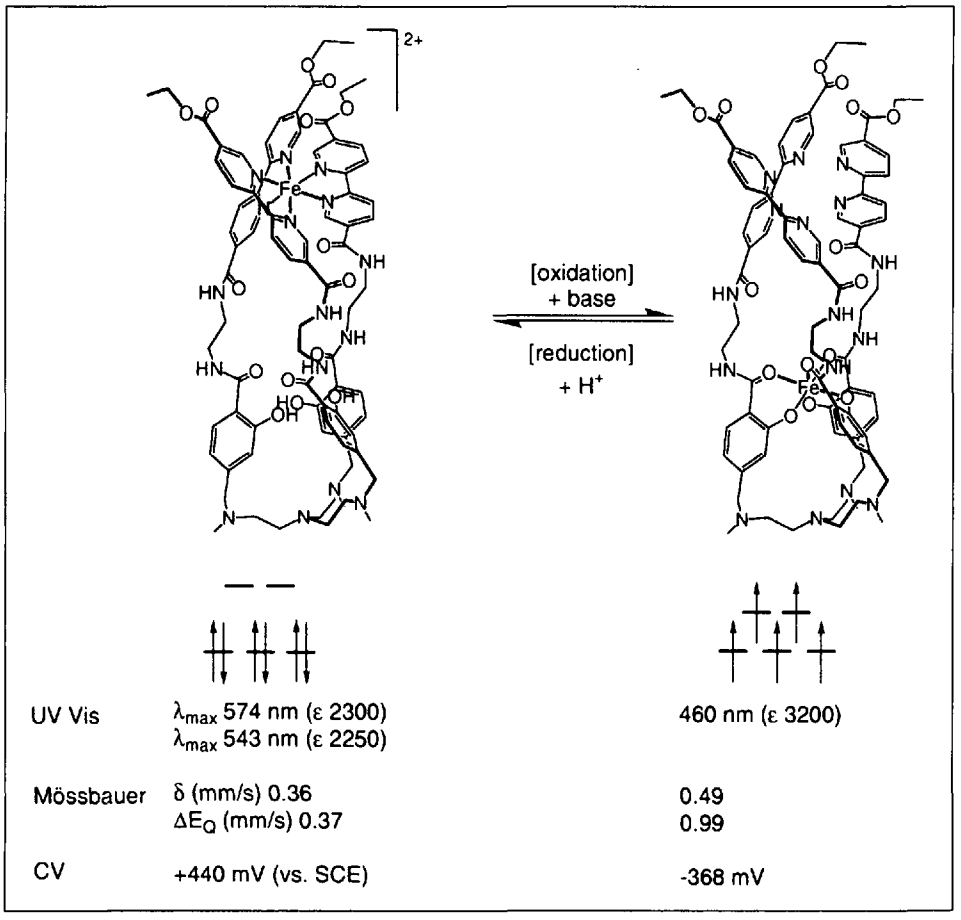

Fig. 12. *Summary of the spectroscopic data of the ferric complex [Fe(III)(NNOO)$_3$] and the ferrous complex [Fe(II)(NNOO)$_3$]$^{2+}$*

general approach for the synthesis of configurationally stable, chiral-at-metal three-legged piano-stool complexes. We are currently testing these as *Lewis* acids in various C–C-bond forming reactions.

– *iii) How is iron released from ferric enterobactin?*

The synthesis of tripodal ligands incorporating salicylamide-binding sites has allowed us to give strong spectroscopic support for the iron release from enterobactin *via* a salicylate binding mode. In addition, we synthesized a fully functional redox-triggered molecular switch. Future directions include inclusion of this device in an artificial membrane as well as a detailed mechanistic investigation of the translocation mechanism.

Herewith I wish to express my gratitude to Prof. Dr. *A. Ludi* as well as the whole faculty of the chemistry and biochemistry department for their unconditional support. This research would not have been possible without the financial support from the *Stiftung für Stipendien auf dem Gebiete der Chemie* (Award of an *A. Werner* Fellowship) as well as the *Swiss National Science Foundation*. I wish to thank my coworkers whose names appear in the publications as well as Prof. Dr. *H.-B. Bürgi* for sharing his passion of science with me.

Received: November 4, 1998

[1] R. Hoffmann, 'The Same and Not the Same', Columbia University Press, New York, 1995.
[2] C. Brändli, T. Ward, *Helv. Chim. Acta* **1998**, *81*, 1616.
[3] T.R. Ward, H.-B. Bürgi, F. Gilardoni, J. Weber, *J. Am. Chem. Soc.* **1997**, *119*, 11974.
[4] J.C. Green, *Chem. Soc. Rev.* **1998**, *27*, 263.
[5] T. Auf der Heyde, *Angew. Chem., Int. Ed. Engl.* **1994**, *33*, 823.
[6] R.D. Wilson, T.F. Koetzle, D.W. Hart, Å. Kvick, D.L. Tipton, R. Bau, *J. Am. Chem. Soc.* **1977**, *99*, 1775.
[7] G. Fachinetti, C. Floriani, F. Marchetti, S. Merlino, *J. Chem. Soc., Chem. Commun.* **1976**, 522.
[8] D. Rüttger, G. Erker, *Angew. Chem., Int. Ed. Engl.* **1997**, *36*, 812.
[9] T.A. Albright, J.K. Burdett, M.-H. Whangbo, 'Orbital Interactions in Chemistry', John Wiley, New York, 1985.
[10] C.J. Piersol, R.D. Profilet, P.E. Fanwick, I.P. Rothwell, *Polyhedron* **1993**, *12*, 1779.
[11] C. Pulham, A. Haaland, A. Hammel, K. Rypdal, H.P. Verne, H.V. Volden, *Angew. Chem., Int. Ed. Engl.* **1992**, *31*, 1464.
[12] T.A. Albright, H. Tang, *Angew. Chem., Int. Ed. Engl.* **1992**, *31*, 1462.
[13] D.L. DuBois, R. Hoffmann, *New J. Chem.* **1977**, *1*, 479.
[14] W.A. Nugent, J. M. Mayer, 'Metal-Ligand Multiple Bonds', John Wiley & Sons, New York 1988.
[15] J.P.L. Ny, M.-T. Youinou, J.A. Osborn, *Organometallics* **1992**, *11*, 2413.
[16] E.L. Muetterties, L.J. Guggenberger, *J. Am. Chem. Soc.* **1974**, *96*, 1748.
[17] R. Bauman, W.M. Davis, R.R. Schrock, *J. Am. Chem. Soc.* **1997**, *119*, 3830.
[18] J.D. Scollard, D.H. McConville, *J. Am. Chem. Soc.* **1996**, *118*, 10008.
[19] U. Siemeling, T. Türk, W.W. Schoeller, C. Redshaw, V.C. Gibson, *Inorg. Chem.* **1998**, *37*, 4738.
[20] B. Therrien, T.R. Ward, *Angew. Chem.* **1998**, in press.
[21] C.G. Frost, J. Horwarth, J.M.J. Williams, *Tetrahedron Asym.* **1992**, *3*, 1089; J. Sprinz, G. Helmchen, *ibid. Lett.* **1993**, *34*, 1769; P. von Matt, A. Pfaltz, *Angew. Chem., Int. Ed. Engl.* **1993**, *32*, 566; A. Togni, U. Burckhardt, V. Gramlich, P.S. Pregosin, R. Salzmann, *J. Am. Chem. Soc.* **1996**, *118*, 1031.
[22] T.V. RajanBabu, A.L. Casalnuovo, *J. Am. Chem. Soc.* **1996**, *118*, 6325.
[23] K. Inoguchi, S. Sakuraba, K. Achiwa, *Synlett* **1992**, 169.
[24] R.D. Adams, D.F. Chodosh, J.W. Faller, A.M. Rosan, *J. Am. Chem. Soc.* **1979**, *101*, 2570.
[25] B.E.R. Schilling, R. Hoffmann, J.W. Faller, *J. Am. Chem. Soc.* **1979**, *101*, 592.
[26] J.A. Gladysz, B.J. Boone, *Angew. Chem., Int. Ed. Engl.* **1997**, *36*, 550.
[27] T.R. Ward, *Organometallics* **1996**, *15*, 2836.
[28] P.E. Blöchl, A. Togni, *Organometallics* **1996**, *15*, 4125.
[29] F. Gilardoni, J. Weber, H. Chermette, T.R. Ward, *J. Phys. Chem., A* **1998**, *102*, 3607.
[30] T.R. Ward, O. Schafer, C. Daul, P. Hofmann, *Organometallics* **1997**, *16*, 3207.
[31] H. Brunner, *Adv. Organomet. Chem.* **1980**, *18*, 151.
[32] P. Hofmann, *Angew. Chem., Int. Ed. Engl.* **1977**, *16*, 536.
[33] E.L. Eliel, S.H. Wilen, L.N. Mander, 'Stereochemistry of Organic Compounds', John Wiley, New York, 1994.
[34] B. Therrien, T.R. Ward, M. Pilkington, C. Hoffmann, F. Gilardoni, J. Weber, *Organometallics* **1998**, *17*, 330.
[35] T.R. Ward, A. Lutz, S.P. Parel, J. Ensling, P. Gütlich, P. Buglyó, C. Orvig, *Inorg. Chem.* submitted.
[36] M. Olumucki, 'The Chemistry of Life', McGraw-Hill, New York, 1993.
[37] E.C. Theil, K.N. Raymond, in 'Bioinorganic Chemistry', Eds. I. Bertini, H.-B. Gray, S.J. Lippard, J.S. Valentine, University Science Books, Mill Valley, California, 1994, p. 1–37.
[38] B.F. Matzanke, G. Müller-Matzanke, K.N. Raymond, in 'Iron Carriers and Iron Proteins', Ed. T.M. Loehr, VCH, Weinheim, 1989, p. 1–121.
[39] A. Lutz, T.R. Ward, *Helv. Chim. Acta* **1998**, *81*, 207.
[40] A. Lutz, T.R. Ward, M. Albrecht, *Tetrahedron* **1996**, *52*, 12197.
[41] For an excellent related report see: L. Zelikovich, J. Libman, A. Shanzer, *Nature (London)* **1995**, *374*, 790.
[42] V.L. Pecoraro, G.B. Wong, T.A. Kent, K.N. Raymond, *J. Am. Chem. Soc.* **1983**, *105*, 4617.
[43] T.R. Ward, S. Duclos, B. Therrien, K. Schenk, *Organometallics* **1998**, *17*, 2490.